

Energy Depletion, Calcium and the Cytoskeleton: A Model for Trophic Intervention

B. T. Stokes, Q. Li, R. A. Altschuld, B. E. Batten and
D. K. Anderson*

The Ohio State University College of Medicine, Columbus, OH 43210;

*University of Cincinnati College of Medicine, Cincinnati, OH 45267

The use of trophic or growth factors to promote regeneration or repair in the injured central nervous system (CNS) presupposes a thorough understanding of the mechanisms by which neurons become injured. The time course and magnitude of this injury process is commonly divided into two principle epochs: acute and secondary. Trophic factors are more likely to provide a protective or nutritive action later in the acute phase simply because plastic reactions of the CNS take time to occur. The trophic effects on secondary degradation on the other hand, are also likely to involve synaptic plasticity and/or frank regeneration of available neural elements. Distinguishing between these possibilities is difficult and will probably require the use of appropriate *in vitro* model systems that can be easily compared with the *in vivo* injury process. It is clear that we have made only limited progress in the past decade in advancing such models and mechanistic explanations of these trophic actions at the cellular level.

This chapter outlines one such approach to a model system in which metabolic injury, calcium homeostasis, and protein metabolism in deenergized cultured spinal neurons are studied in the same population of cells. As such, it provides a way to examine important hypotheses that attempt to relate the process of energy depletion to structural alterations after the ischemic insult when the potential for reversal is likely to be the greatest. In addition, because the mechanisms of action of such factors as gangliosides (see Ledeen, *this symposium*) are likely to be exerted via alterations in calcium metabolism, it also provides a relevant cellular model in which to address these pharmacological issues.

ENERGY METABOLISM AND CELL INJURY

Injury to neuronal cells is associated with a decline in high energy phosphates, a loss of cation homeostasis, and possibly, an increase in reactive oxygen radicals.

In ischemia, but possibly not hypoglycemia, there is also a decline in cellular pH. The exact linkage between these events and the physiologic and pathologic sequelae of neuronal injury at the cellular level, particularly in the spinal cord, has not been clearly defined (recent reviews of these issues include 4,32,39,40). The pH changes are of some importance because the relative sodium load precipitated by energy depletion will affect membrane Na^+/H^+ exchangers and thus indirectly affect operation of $\text{Na}^+/\text{Ca}^{+2}$ exchanger on the cell membrane. Relative alterations in pH may also affect sodium loading during deenergization.

It is now clear that a variable rate of energy depletion is characteristic of ischemic or traumatically induced spinal cord injury. Within 5 min after cord contusion injury, ATP levels and energy charge have fallen to a fraction of their control values (19,36,37), particularly in the grey matter (38). During spinal ischemia a more gradual decline in these reserves takes place and energy metabolites respond quickly to the restoration of control conditions (2,12). Corresponding alterations in other of the adenine nucleotide metabolites have been examined (32,33) that seem to mimic the known chemistry of these pathways in the cerebrum (31). Interestingly, after electrical shock, adenine nucleotide degradation in the rat brain seems to occur preferentially via adenylate deaminase; but during ischemia, dephosphorylation of AMP appears to be the dominant pathway. In both cases, however, there is a net decline in the size of the adenylate pool and an increase in adenosine, inosine, and hypoxanthine.

The rapidity with which ATP loss occurs in the traumatized spinal cord can also be mimicked in culture preparations (Fig. 1). Here we have shown that cultured spinal neuronal cells lose ATP and total adenine nucleotides when challenged with amytal (A) and carbonyl cyanide m-chlorophenyl hydrazone (CCP); these are a NADH dehydrogenase inhibitor and a proton ionophore, respectively. This is associated with an increase in ADP and AMP as the total nucleotide pool falls. Upon removal of these compounds, there is a rebound in ATP toward control values with a concomitant decrease in the ADP pool; the size of the total adenine nucleotide pool, however, remains depressed. The loss of total adenylates in these protocols most likely involves the production and cellular efflux of adenosine, inosine, and hypoxanthine. However, cell death in a fraction of the population could also cause a decline in measured adenine nucleotides. In addition, the incomplete recovery of ATP/ADP in these protocols may be explained by intracellular compartmentalization of ADP rather than a true decline in the adenylate charge of the cytosol. It is clear that we are able to mimic many characteristics of the energy depletion known to occur *in situ* elsewhere in the central nervous system (32). Cellular homeostasis, in particular calcium and protein metabolism, are likely to be affected by such alterations.

THE CALCIUM HYPOTHESIS AND NEURONAL CELL INJURY

Cellular calcium metabolism has been extensively reviewed (32) and many features are similar in a variety of cell types (26,32). Ca^{2+} is maintained at low values

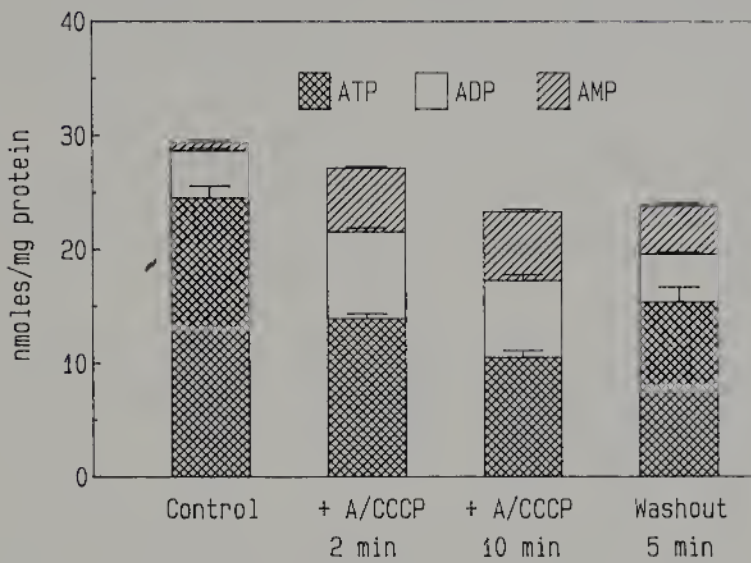


FIG. 1. Energy depletion and adenine nucleotides in culture. Cells were harvested from cultures after freezing with liquid nitrogen, homogenized, and processed for high pressure liquid chromatography (HPLC) as before (18). Cells were also assayed for total protein and results are expressed as nmol of metabolites/mg protein. Cultures were sampled at 2 and 10 min after A/CCCP incubation and 5 min post-incubation (washout). Crosshatched area represents ATP changes, open area ADP, and left-diagonal AMP; mean \pm SEM. The total height of the bars indicates the total adenine nucleotide pool.

($10^{-7}M$) in the cytosol; it can enter via voltage or agonist-dependent channels and reversal of the Na/Ca exchanger. It is reexported after receptor or voltage activation at the expense of metabolic energy. Such energy is either in the form of ATP or the sodium gradient which operates the forward mode of the Na/Ca exchanger. Modes of intracellular regulation of free Ca^{2+} in neuronal cells are also similar to other excitable cells in that active mitochondria, endoplasmic reticulum, and a series of calcium-binding proteins all play a qualitatively similar role in maintenance of these critically low $[Ca^{2+}]_i$ levels (14,32 provide detailed reviews). A marked disturbance of this intracellular calcium homeostasis has become one of the basic tenets of the calcium-neuronal damage hypothesis (6,39,40). Major questions, however, remain about elements of this postulate.

The first relates to the magnitude of the $[Ca^{2+}]_i$ change in individual cells during procedures that mimic cerebral ischemia. Such a question is of some importance if one is to assess the role of intracellular buffering mechanisms during pathological processes. We also do not know whether the diminution of extracellular free calcium, which has been repeatedly described during injury or ischemia in the CNS (6,39), contributes to a calcium paradox phenomenon (39) in the acutely uninjured

neuron population. Without a precise knowledge of the time course of such phenomena, one cannot establish a causal relationship between Ca^{2+} entry and subsequent pathological events. The uncertainty of such information continues to be one of the primary problems with the calcium neurotoxicity hypothesis (11,40). Careful attention must also be paid in any cell line to quantitation of the change in $[\text{Ca}^{2+}]_i$ when measurements of intracellular free Ca^{2+} are made in injury or events that mimic cellular ischemia. As discussed below, we have used the fluorescent Ca^{2+} indicator fura-2 in single cells and carefully estimated the potential contributors to the Ca^{2+} -sensitive signal of fura-2.

INTRACELLULAR CALCIUM DYNAMICS AS MEASURED BY FURA-2 TECHNOLOGY

The accurate characterization of the free Ca^{2+} transients in single cells has been dependent on the recent development of fluorescent probes (e.g., fura-2) that allow the necessary fast time resolution without the non-linearity or potential cell damage that may exist with other techniques (e.g., aequorin or Ca^{2+} -selective microelectrodes, 17). The acetoxyethyl ester form of this Ca^{2+} -sensitive probe (fura-2/AM), developed by Tsien and his colleagues (17,35), can be easily incorporated into the cell and deesterified by intracellular esterases to form the Ca^{2+} -sensitive acid moiety. The high fluorescence yield of fura-2 also permits detection of the signal from a small amount of intracellular dye and thus reduces the potential buffering capacity. The dye is sensitive over the range of calcium values that occur during energy depletion protocols (at least to 5–10 μM), shows little interference by competing ions, and does not overtly interfere with normal cell function. We have previously used fura-2/AM to calibrate and characterize the slow $[\text{Ca}^{2+}]_i$ changes that occur in cardiac myocytes after energy depletion (21–24). By using the characteristic shift in fura-2 excitation spectra upon binding Ca^{2+} and the associated ratio techniques (35) that theoretically eliminate many of the problems (dye bleaching, changes in cell geometry or pathlength, etc.) found with previous fluorescent dyes of this type (e.g., quin-2), accurate characterization of Ca^{2+} transients can be achieved (17,35). The use of such probes is not, however, without potential problems.

The major problems with the use of fluorescent dyes lie in the areas of calibration of the dye signals because of intracellular compartmentalization and/or incomplete deesterification. Our work in energy-depleted cardiac myocytes has provided a method to correct for the highly fluorescent but calcium-insensitive dye components formed by incomplete dye deesterification (22,23). Such studies have produced reliable agreement between *in vivo* and *in vitro* calibration curves under a variety of conditions (23,30). In addition, we have estimated the contribution of the mitochondrial pool to our fluorescence signal after deenergization (13). Finally, it is also clear that excess dye loading can significantly impair intracellular calcium

dynamics (1,3,20,34). By appropriate control of loading procedures (1,3,29), however, such artifacts can be minimized if not eliminated. Under these carefully defined conditions, calcium-induced shifts in fura-2 fluorescence can be used to accurately describe slow and fast calcium transients with reliable accuracy.

Measurement of Intracellular free Ca^{2+} in Single Cells: System Design

We have used a PTI Deltascan system to achieve sufficient sensitivity and temporal resolution of the calcium dynamics. It essentially allows the fast time and dual-excitation fluorescence measurements necessary to accomplish different experimental protocols with our cell populations. Excitation wavelengths in the system are provided by a 75W xenon lamp through two excitation monochrometers set at 350 and 380 nm, respectively. The two excitation wavelengths are alternated at 100 Hz (variable; operator selected) by a motor-controlled spinning chopper similar to that described by Danielisova et al. (12). The light beam from either of these sources is directed into the light path of the inverted microscope equipped with a 63X Plan-Neofluar objective, which focuses on the specimen. Emission (420–620 nm) at the two excitation wavelengths from the cell is collected by a photomultiplier tube (PMT). A dichroic mirror (Zeiss FT395) is used to separate the excitation and emission components between the objective and the PMT. The computer program synchronizes the PMT sample mode with the chopper rate to store signals from the two excitation wavelengths into two different channels without crosstalk. Resident programs are used to collect the emission data, plot it in single or dual channel modes, data average, or construct ratios that are used to estimate free calcium. The entire optical path to and from the cell (with the exception of the coverslip at the bottom of the chamber) is through quartz elements to maximize UV transmission and avoid shifts of excitation spectra to higher wavelengths. This is necessary to increase system sensitivity at the low loading magnitude needed to avoid fura-2 buffering (24).

A single cell is placed in the UV-illuminated field (adjusted by a diaphragm) of the 63X objective to avoid signal contamination from neighboring cells. To minimize UV exposure of the cell, a computer-controlled shutter is placed on the excitation side of the light path and is opened only when measurements are being made.

Calcium Dynamics and Energy Depletion

Our previous experience with energy depletion paradigms (10,21,24,28) in other cell lines and use of the fura-2 technology allowed us to examine the consequences of deenergization in our primary culture model.

In a series of spinal cord ventral horn cultures treated in a similar manner with

A/CCCP, we have repeated some of our earlier protocols (21,22,23). From such measurements we estimate the resting free calcium in these cells to be significantly lower ($n = 7$; $150 - 300 \text{ nM}$) than values found with ion-sensitive microelectrodes but in agreement with other non-invasive techniques (26).

In Fig. 2 and Fig. 3, individual culture plates were loaded with $2 \mu\text{M}$ fura-2/AM for 5–10 min at room temperature and post-incubated for 1–2 hr. The low concentration and short loading time of the dye are used to minimize the large uptake of fura-2/AM by the cells and the consequent calcium buffering by the deesterified fura-2. Post-incubation is necessary to insure maximal hydrolysis of the fura-2 ester form, which is critical for accurate calibration of the fluorescence signal.

In Figure 2, we show the effects of energy depletion on a single cell. The effects are quite dramatic because free calcium exceeds $10 \mu\text{M}$ several minutes after ex-

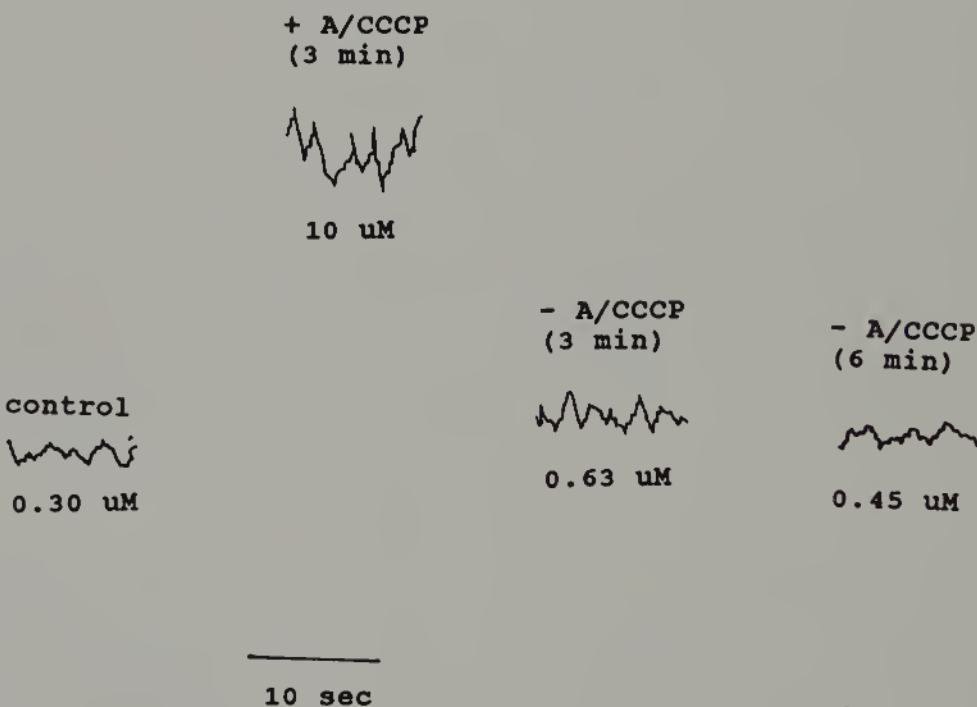
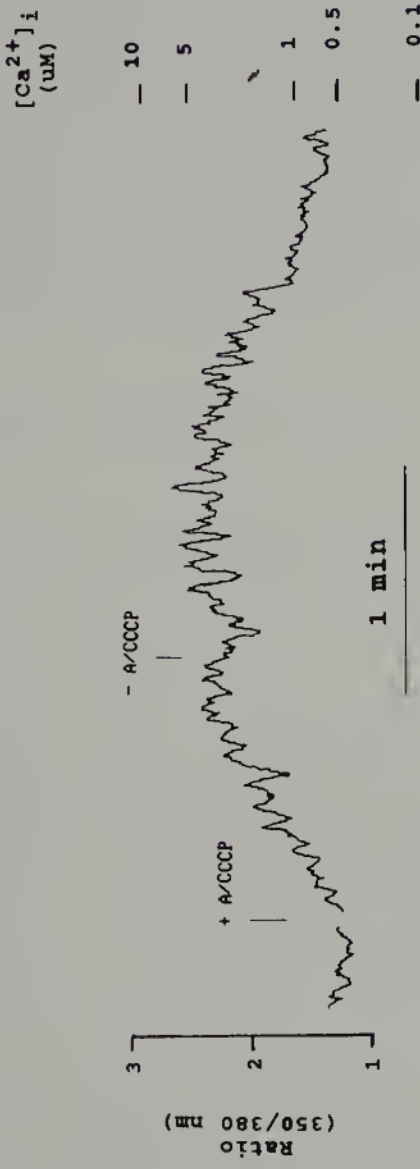


FIG. 2. Changes in intracellular free Ca^{2+} by metabolic inhibition. Fura-2-loaded cultured neurons were bathed in a closed perfusion chamber and continuously perfused with Krebs-Henseleit (K-H) bicarbonate buffer at 35°C , pH 7.3. Metabolic inhibition was achieved by perfusing the cells with K-H buffer containing 3 mM amytal and $2 \mu\text{M}$ CCCP (A/CCCP). The fluorescence signal from a single neuron was measured at times indicated. The Ca^{2+} -saturated and Ca^{2+} -free fura-2 signals were determined intracellularly at the end of the experiment and the fluorescence ratio was converted to $[\text{Ca}^{2+}]_i$ as described (22). The absolute estimations of $[\text{Ca}^{2+}]_i$ appear below each of the traces.

2ND EXPOSURE



4TH EXPOSURE



FIG. 3. Effects of energy depletion and subsequent repletion from the same cell after repeated exposure. Traces from the 2nd and the 4th of such protocols are shown. Notice the further increase in $[Ca^{2+}]_i$ upon washout before the recovery.

posure. Reversal of these effects is evident as calcium quickly returns to near normal levels within 3 and 6 min after drug removal. This rate of increase is considerably faster than that which occurs in other energy-depleted cell lines as is the ability to quickly exclude the excess free calcium (21–24). In those cells studied ($n = 9$), intracellular calcium quickly rose to over $2 \mu\text{M}$ within 3 min as a result of the energy depletion paradigm.

In Figure 3, we document the effects of repeated exposure to such regimens. Conceptually, such treatments might be related to intermittent reperfusion phenomena that occur in the injured CNS. Note the delayed recovery during the second exposure as calcium continues to rise after reenergization. Such increases may result from release of calcium from overloaded intracellular stores. Notice also that repeated exposures progressively produce higher calcium levels in the same cell (4th exposure), particularly during recovery from the insult. Further disturbance of intracellular organelles may also contribute to this pattern. Future experiments are needed to establish the mechanisms by which such dynamics in $[\text{Ca}^{2+}]_i$ take place after reenergization and if "calcium paradox" phenomena occur in cultured neurons.

The final element in the calcium hypothesis is of course to provide some dynamic measure of structural alterations that may occur in the cultured neurons as a result of energy depletion and the consequent elevations in intracellular free calcium.

THE NEURONAL CYTOSKELETON AND CALCIUM METABOLISM

General Aspects of the Neuronal Cytoskeleton

The neuronal cytoskeleton is comprised of three fibrous elements: microfilaments (MF), neurofilaments (NF), and microtubules (MT) (8). The major polypeptide components of these substructures have been examined in detail. MFs are polymers of actin with associated actin-regulator proteins. NFs consist of three polypeptides of molecular weights 200,000, 150,000, and 70,000 and microtubules are polymers formed from the heterodimer α and β tubulin with associated proteins, ie., microtubule-associated proteins (MAPs). The complex interaction of these various components is critical to the maintenance of the great variety of forms illustrated by the hundreds of distinguishable cell types in the vertebrate nervous system.

The intrinsic form and function of the neuronal cytoskeleton is imparted by the associated regulatory proteins such as actin-binding proteins and MAPs. It is not surprising that the organization of the axonal and dendritic cytoskeleton is very different (9). The cell body, which is the site of synthesis of neuronal proteins, is a mixture of both axonal and dendrite-specific cytoskeletal protein. Actin microfilaments are found throughout the neuron; however, actin-binding proteins such as the spectrin isoforms (fodrin) are localized either exclusively in the axon or dendrite. Microtubules are components of all processes, however, tyrosinated α tubulin is dendrite specific and acetylated α tubulin is axon specific. This is further complicated by the varied distribution of the MAPs (9).

Calcium and the Neuronal Cytoskeleton

Virtually all components of the cytoskeleton are either directly or indirectly affected by alterations in calcium metabolism (25). Furthermore, increasing evidence indicates that calcium-activated proteases may also specifically modulate components of the cytoskeleton (15,27). In this regard, calcium-dependent proteases have been implicated in spinal damage and shown to be associated with extensive total calcium accumulation in the hours after traumatic insult (5). In addition to the Ca^{2+} -sensitivity of cytoskeleton, it has also been well-established that actin is an ATP-binding protein (25) and several of the actin regulatory proteins are ATP-dependent (25). Thus ATP depletion itself may directly alter the structural components of the neuronal cytoskeleton. It is of interest to point out that numerous major neurodegenerative diseases such as Alzheimer's, Parkinsonian syndrome, amyotrophic lateral sclerosis, as well as a variety of toxic neuropathies are also characterized by changes in the neuronal cytoskeleton (7,16).

Confocal Microscopy as a Tool to Investigate the Problem

A BioRad Lasersharp MRC-500 scanning laser confocal microscope has been used to conduct the studies on the structural correlates of neuronal deenergization. The MRC-500 converts the standard research microscope into a laser scanning confocal system. Designed particularly for applications in fluorescence microscopy, the system is provided with a multi-line argon ion laser able to excite many commonly used fluorochromes such as fluorescein, rhodamine, and Texas red. In addition, operation is also possible at all reflective wide bandpass optics; the transfer system is thus fully achromatic at all wavelengths from UV to near infrared.

The MRC-500 is controlled by a Nimbus VT desktop computer with purpose-built cards for controlling scanning and image acquisition. The computer-driven focus control allows for optical sectioning. A second independent detector can be used to detect transmitted phase, bright field or Nomarski, and epifluorescence or reflectance microscopy. The software has functions for either displaying the two images simultaneously or "merging" them for direct comparison.

The key element of confocal optics is a spatial filter situated in the reflected light path. The filter is configured so that the region viewed at any one time is coincident with the diffraction-limited illuminating spot. Thus, illumination and detection apertures are "confocal" with each other. The advantage over the conventional microscope is that only a single focal plan is illuminated at any one time.

The confocal optical system dramatically changes the contrast properties of the optical microscope. Only those regions of the sample lying within a narrow focal plane are imaged. Regions above and below this plane appear black rather than blurred as in the conventional system. As a result, contrast is not degraded by out of focus flare and it is possible to obtain images with extraordinary clarity and detail. In addition, the acquisition of accurate quantitative data is possible because

of the exclusion of signals from out of focus regions in the tissue cultures. This instrument has been used to assess protein alterations as described below.

Energy Depletion and Confocal Microscopy

In Figure 4, we have illustrated the distribution of F-actin in control cultures with the F-actin-specific probe rhodamine phalloidin; (A) phase-contrast transmitted image, (B) confocal image of rhodamine-phalloidin fluorescence. Actin staining in neurons was most concentrated in the cell body, densitometric quantitation of fluorescence revealed that more staining was evident in the cell body (26.4) when compared to the processes (22.1). Actin filament bundles (stress fibers) can also be seen to be prominent features of the non-neuronal cells present in these cultures. In this particular plane of section, the non-neuronal cells (below and left of the neuron) stain more intensely than the neurons (30.00).

Figure 5 is an example (A and B as in Fig. 4 above) of actin-staining patterns in cells that had been ATP-depleted. Actin appears to be clumped into aggregates

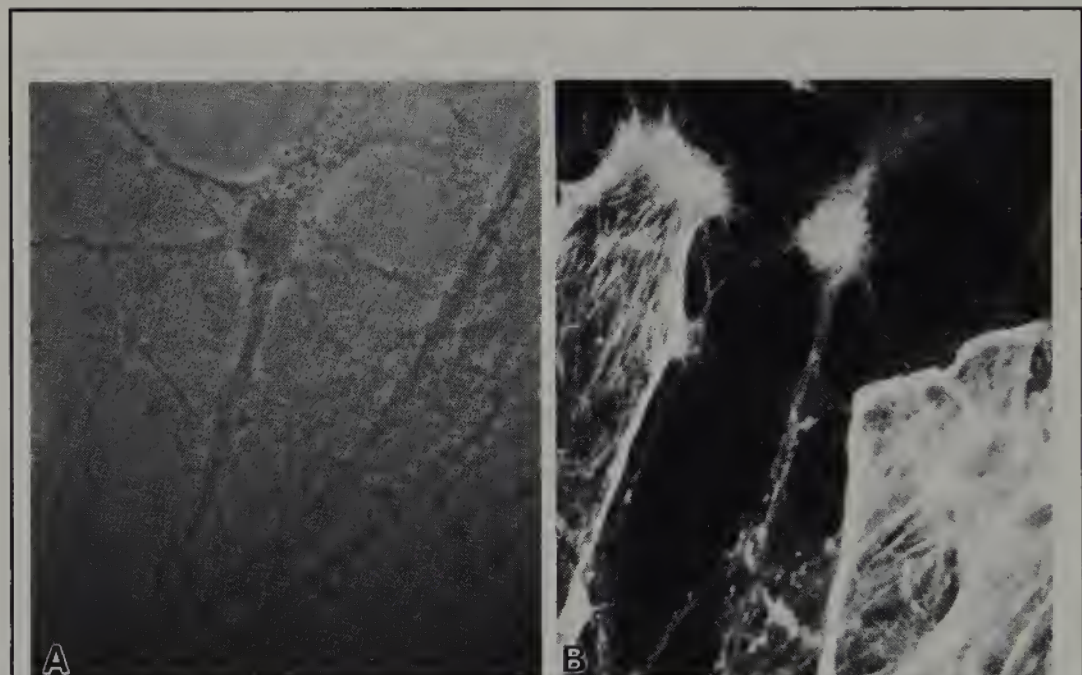


FIG. 4. Illustration of the distribution of F-actin in control cells from primary ventral-horn cultures. In the phase contrast image (A), a single neuron is evident with several flattened cell profiles (presumably astrocytes) slightly out of the plane of focus. F-actin staining in the same plane of section (B) reveals a dense distribution of the label in neural and non-neuronal elements.

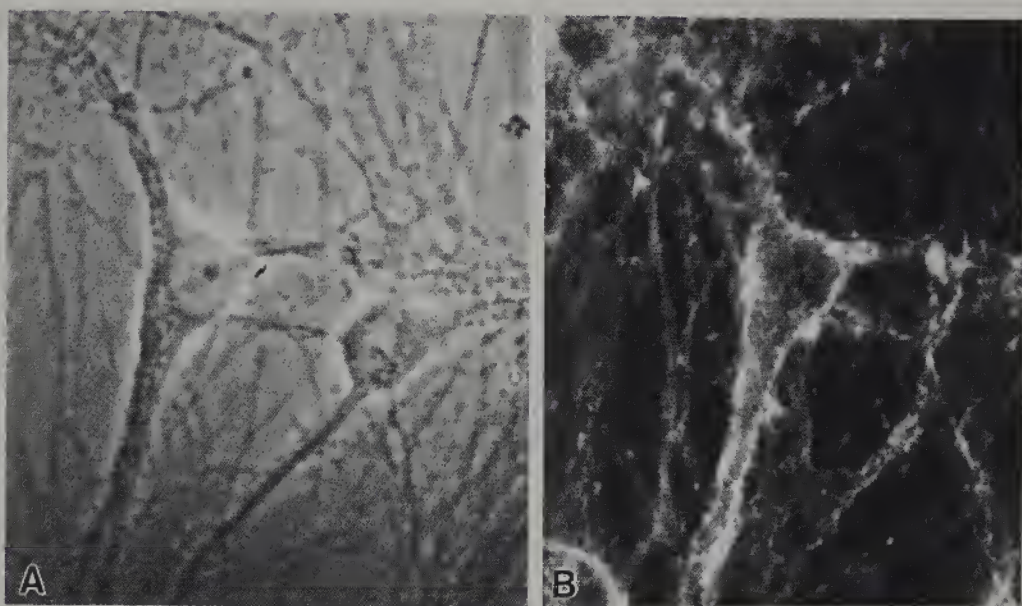


FIG. 5. F-Actin distribution in energy-depleted cells from ventral-horn cultures. Cultured cells (**A**-phase contrast) were energy depleted for 10 min as before (see above), fixed and stained for F-actin (**B**). Energy depletion caused a remarkable decrease in cytosolic F-actin.

along the neuron plasma membrane but markedly decreased in the neuronal perikaryon. Actin in non-neuronal cells did not appear to be distributed differently from controls. Quantitative measurements of actin staining revealed that F-actin levels were lower in ATP-depleted neurons (16.3 whole cell, 15.6 cell body, and 12.4 for the processes). Actin measurements of non-neuronal cells, however, were similar to controls. Such measurements are quite repeatable and revealed the power of using confocal microscopy to discriminate between types and individual cell processes.

SUMMARY

We have outlined an approach to a model system in which the investigation of growth factors may take place. In particular, we have conducted experiments that reveal the neurochemical alterations produced by energy depletion in neural cultures. By coupling these to the free calcium estimations and structural degradation (revealed by the confocal microscope), we are able to add mechanistic arguments

to the calcium-neurotoxicity hypothesis. This is particularly true when free calcium exceeds the necessary levels to activate neutral proteases in the cell interior. Future experiments of this type, and the intervention with protocols designed to ameliorate the ensuing pathological process, will undoubtedly result in more clearly defined hypotheses of how neuronal toxicity occurs.

REFERENCES

1. Almers W, Neher E. The Ca signal from fura-2 loaded mast cells depends strongly on the method of dye-loading. *FEBS. Lett.* 1985;192:13-18.
2. Anderson DK, Behbehani MM, Means ED, Waters TR, Green ES. Susceptibility of feline spinal cord energy metabolism to severe incomplete ischemia. *Neurology* 1983; 33:722-731.
3. Ashley CC, Potter JD, Strang P, Godber J, Walton A, Griffiths PJ. Kinetic investigations in single muscle fibers using luminescent and fluorescent Ca^{2+} probes. *Cell Calcium*. 1985;6:159-181.
4. Balazs R. Metabolic imbalance and nerve cell damage in the brain. *Prog. Brain. Res.* 1988;73:447-463.
5. Banik NL, Hogan EL, Powers JM, Whetstine LJ. Degradation of cytoskeletal proteins in experimental spinal cord injury. *Neurochem. Res.* 1982;7:1465-1475.
6. Beattie MS, Stokes BT. Experimental spinal cord injury: strategies for acute and chronic intervention based on anatomic, physiologic and behavioral studies. In: Stein DG, Sabel BA, eds. *Pharmacologic Approaches to the Treatment of Brain and Spinal Cord Injury*. New York: Plenum Publishing Corp., 1988;59-72.
7. Binet S, Meininger V. Modifications of microtubule proteins in ALS nerve precede detectable histologic and ultrastructural changes. *Neurology* 1988;38:1596-1600.
8. Bray D, Gilbert D. Cytoskeletal elements in neurons. *Annu. Rev. Neurosci.* 1981; 4:505-523.
9. Burgoyne RD, Cambray-Deakin MA. The cellular neurobiology of neuronal development: the cerebellar granule cell. *Brain. Res.* 1988;472:77-101.
10. Caciagli F, Ciccarelli R, Dilorio P, Ballerini P, Tacconelli L. Cultures of glial cells release purines under field electrical stimulation: the possible ionic mechanisms. *Pharm. Res. Comm.* 1988;20(11):935-947.
11. Cheung JY, Bonventre JV, Malis CD, Leaf A. Calcium and ischemic injury. *N. Engl. J. Med.* 1986;314:1670-1676.
12. Danielisova V, Chavko M, Kehr J. Adenine nucleotide levels and regional distribution of ATP in rabbit spinal cord after ischemia and recirculation. *Neurochem. Res.* 1987; 12:241-245.
13. Davis MH, Altschuld RA, Jung DW, Brierley GP. Estimation of intramitochondrial pCa and pH by fura-2 and 2,7-biscarboxyethyl-5(6)-carboxyfluorescein (BCECF) fluorescence. *Biochem. Biophys. Res. Commun.* 1987;149:40-45.
14. DiPolo R, Beauge L. Ca^{2+} transport in nerve fibers. *Biochem. Biophys. Acta* 1988; 947:549-569.
15. Gallant PE, Pant HC, Pruss RM, Gainer H. Calcium-activated proteolysis of neurofilament proteins in the squid giant neuron. *J. Neurochem.* 1986;46:1573-1581.

16. Goldman JE, Yen SH. Cytoskeletal protein abnormalities in neurodegenerative diseases. *Ann. Neurol.* 1986;20:9–223.
17. Grynkiewicz G, Poenie M, Tsien RY. A new generation of Ca^{2+} indicators with greatly improved fluorescence properties. *J. Biol. Chem.* 1985;260:3440–3450.
18. Hammer DF, Unverferth DV, Kelley RE, Harvan PA, and Altschuld RA. Extraction and measurement of myocardial nucleotides, nucleosides, and purine bases by high-performance liquid chromatography. *Anal. Biochem.* 1988;169:300–305.
19. Hayashi N, Tsubokawa T, Green BA. Changes in energy metabolism and spinal cord blood flow following severe spinal cord injury. *No. Shinkei. Geka.* 1984;12:923–930.
20. Lambert MR, Johnson JD, Lamka KG, Brierley GP, Altschuld RA. Intracellular free Ca^{2+} and the hypercontracture of adult rat heart myocytes. *Arch. Biochem. Biophys.* 1986;245:426–435.
21. Li Q, Altschuld RA, Biagi BA, Stokes BT. Cation and membrane potential alterations in energy depleted cardiac myocytes. In: Clark WA, Decker RS, Borg TK, eds. *Biology of Isolated Adult Cardiac Myocytes*. New York: Elsevier Science Publishing Co., 1988; 342–345.
22. Li Q, Altschuld RA, Stokes BT. Quantitation of intracellular free calcium in single adult cardiomyocytes by fura-2 fluorescence microscopy: calibration of fura-2 ratios. *Biochem. Biophys. Res. Commun.* 1987;147:120–126.
23. Li Q, Altschuld RA, Stokes BT. Myocyte deenergization and intracellular free calcium dynamics. *Am. J. Physiol.* 1988;255:C162–C168.
24. Li Q, Hohl CM, Altschuld RA, Stokes BT. Energy depletion/repletion and calcium transients in single cardiomyocytes. *Am. J. Physiol.* 1989;257(Cell Physiol. 26):C427–C434.
25. Mooseker MS. Organization, chemistry, and assembly of the cytoskeletal apparatus of the intestinal brush border. *Annu. Rev. Cell Biol.* 1985;1:209–241.
26. Morris ME, Friedlich JJ, MacDonald JF. Intracellular calcium in mammalian brain cells: fluorescence measurements with quin2. *Exp. Brain. Res.* 1987;65:520–526.
27. Nixon RA. Fodrin degradation by calcium-activated neutral proteinase (CANP) in retinal ganglion cell neurons and optic glia: preferential localization of CANP activities in neurons. *J. Neurosci.* 1986;6:1264–1271.
28. Panula P, Emson P, Wu JY. Demonstration of enkephalin-, substance P- and glutamate decarboxylase-like immunoreactivity in cultured cells derived from newborn rat neostriatum. *Histochemistry.* 1980;69:169–179.
29. Peeters GA, Hlady V, Bridge JH, Barry WH. Simultaneous measurement of calcium transients and motion in cultured heart cells. *Am. J. Physiol.* 1987;253:H1400–H1408.
30. Scanlon M, Williams DA, Fay FS. A Ca^{2+} -insensitive form of fura-2 associated with polymorphonuclear leukocytes. Assessment and accurate Ca^{2+} measurement. *J. Biol. Chem.* 1987;262:6308–6312.
31. Schultz V, Lowenstein JM. The purine nucleotide cycle. Studies of ammonia production and interconversions of adenine and hypoxanthine nucleotides and nucleosides by rat brain *in situ*. *J. Biol. Chem.* 1978;1938–1943.
32. Siesjo BK. Historical overview. Calcium, ischemia, and death of brain cells. *Ann. N.Y. Acad. Sci.* 1988;522:638–661.
33. Siesjo BK. Hypoglycemia, brain metabolism, and brain damage. *Diabetes. Metab. Rev.* 1988;4:113–144.
34. Thomas AP, Selak M, Williamson JR. Measurement of electrically induced Ca^{2+} transients in Quin2-loaded cardiac myocytes. *J. Mol. Cell Cardiol.* 1986;18:541–545.

35. Tsien RY, Rink TJ, Poenie M. Measurement of cytosolic free Ca^{2+} in individual small cells using fluorescence microscopy with dual excitation wavelengths. *Cell Calcium*. 1985;6:145–157.
36. Vink R, McIntosh TK, Weiner MW, Faden AI. Effects of traumatic brain injury on cerebral high-energy phosphates and pH: a ^{31}P magnetic resonance spectroscopy study. *J. Cereb. Blood Flow. Metab.* 1987;7:563–571.
37. Vink R, McIntosh TK, Yamakami I, Faden AI. ^{31}P NMR characterization of graded traumatic brain injury in rats. *Magn. Reson. Med.* 1988;6:37–48.
38. Walker JG, Yates RR, Yashon D. Regional canine spinal cord energy state after experimental trauma. *J. Neurochem.* 1979;33:397–401.
39. Young W. Ca paradox in neural injury: a hypothesis. *CNS Trauma* 1986;3:235–251.
40. Young W. The post-injury responses in trauma and ischemia: secondary injury or protective mechanisms? *CNS Trauma* 1987;4:27–51.